Title
A Multifrequency Phase Fluorometer Using the Harmonic Content of a Mode-Locked Laser

Journal
Instrumentation Science & Technology, 14(3-4)

ISSN
1073-9149

Authors
Alcala, J Ricardo
Gratton, Enrico
Jameson, David M

Publication Date
1985

DOI
10.1080/10739148508543579

ANALYTICAL INSTRUMENTATION, 14(3&4), 225-250 (1985)

A MULTIFREQUENCY PHASE FLUOROMETER USING THE HARMONIC CONTENT OF A MODE-LOCKED LASER

J. Ricardo Alcala, Enrico Gratton*

Department of Physics
University of Illinois at Urbana-Champaign
1110 West Green Street, Urbana, IL 61801

David M. Jameson

Pharmacology Department
University of Texas Health Science Center
5323 Harry Hines Blvd., Dallas, TX 75235

ABSTRACT

We describe the construction and operation of a cross-correlation phase and modulation fluorometer which uses the harmonic content of a high repetition rate mode-locked laser as the excitation source.

A mode-locked argon ion laser is used to synchronously pump a dye laser. The pulse train output from the dye laser is amplitude modulated by an acousto-optic modulator and then frequency doubled with an angle tuned frequency doubler. With the particular dye utilized in these studies, the ultraviolet light obtained was continuously tunable over the range 280-310 nm. In the frequency domain the high repetition rate pulsed source gives a large series of equally spaced harmonic frequencies. The frequency spacing of the harmonics is determined by the repetition frequency of the laser. Amplitude modulation of the pulse train permits variation of the frequency quasi-continuously from a few hertz to gigahertz. Use of cross-correlation techniques permits precise isolation of individual frequencies. The cross-correlation frequency required

 0743-5797/85/1403-0225$3.50/0

for the analysis of the phase delay and modulation ratio is obtained using coupled frequency synthesizers. In the present instrument three synthesizers are used. One drives the pump mode-locker head, a second drives the acousto-optic modulator and the third is used to modulate the response of the photomultiplier tubes which detect the signal. The accuracy, reproducibility and sensitivity of the instrumentation have been determined. Experimental data are provided to show use of this high frequency cross-correlation phase-modulation fluorometer for the determination of fluorescence lifetimes and rotational motions of tryptophan in solution and in proteins.

1. INTRODUCTION

In recent years there has been a marked interest in the use of fluorescence spectroscopy for the study of dynamics of macromolecules. The natural time window of fluorescence is suitable to resolve events occurring in the nanosecond-subnanosecond time domain. In particular, the intrinsic fluorescence of proteins, due primarily to the tryptophan and tyrosine residues, have been extensively investigated as probes of dynamic processes. Even proteins containing a single tryptophan or tyrosine emitter, however, may demonstrate complex decay schemes, i.e., heterogeneity may exist in the lifetime as well as rotational modes of the fluorophore.[1-3] The practical utility of fluorescence methods is thus still limited by the availability of instrumentation capable of measuring such events accurately and resolving the heterogeneity. Our particular interest has been the development of multifrequency phase fluorometry and especially its application to the study of subnanosecond macromolecular dynamics using intrinsic fluorescence probes such as tryptophan and tyrosine residues.

A multifrequency phase and modulation fluorometer capable of picosecond resolution has been described[4] and operational in our laboratory for a number of years. This instrument performs well using the visible and UV lines from a CW laser source (either

argon-ion or helium-cadmium) and a Pockels cell for modulation. However, the poor performance of Pockels cells in the UV, their limited frequency response and the lack of convenient CW UV sources motivated the present work.

In this paper we present (i) the theoretical basis for use of a mode-locked laser as an excitation source for phase and modulation fluorometry, (ii) details of the construction and operation of the instrument, and (iii) results on systems of biophysical interest. The instrument achieves clear resolution of heterogeneous fluorescence lifetimes and measures fluorescence anisotropy decays in the subnanosecond-nanosecond time scale. The exciting modulation frequencies are variable quasi-continuously from a few Hz to one GHz.

2. THEORY

The time decay of fluorescence is typically measured using one of two different approaches. The system response to transient (pulsed) excitation can be determined in the time domain by the popular technique of time correlated single photon counting.[5] Alternatively, the fluorescence response can be measured in the frequency domain, using a light source with an intensity which is modulated sinusoidally, by determining the phase delay and the relative modulation of the fluorescence signal with respect to the exciting light. The time domain and frequency domain approaches provide equivalent information and are related to each other by the fourier transform. The basic relations between the time response and the frequency response have been given by Weber[6] and are discussed below for the reader's convenience.

In the time domain the response to the delta function excitation of an emitting system comprising N exponentially decaying components is given by the following equation,

$$I_f(t) = \sum_{i=1}^{N} \alpha_i e^{-t/\tau_i}. \qquad (1)$$

In the frequency domain the time variation of the excitation light intensity is described by

$$E(t) = E_o(1 + M_e \sin \omega t) \tag{2}$$

where E_o and M_e are the average value of the intensity and the modulation of the excitation respectively. The overall fluorescence response of the system to the sinusoidal excitation can be written in the form

$$F(t) = F_o[1 + M_f \sin(\omega t - \phi)]. \tag{3}$$

Where F_o and M_f are the average value of the intensity and the modulation of the fluorescence, respectively. For linear systems the emitted fluorescence has the same modulation frequency but is demodulated and phase-shifted with respect to the exciting light. The phase delay and modulation ratio between the excitation and the emission constitute the two independent measurable quantities in phase fluorometry. The following equations relate these parameters to the case of the pulse response, $I_F(t)$, to excitation by a delta function at excitation frequency, ω,

$$\tan \phi = \frac{S}{G} \tag{4}$$

$$M = \frac{M_f}{M_e} = N^{-1}(S^2 + G^2)^{1/2} \tag{5}$$

where

$$S = \int_o^\infty I_F(t) \sin \omega t \, dt \tag{6}$$

$$G = \int_o^\infty I_F(t) \cos \omega t \, dt \tag{7}$$

$$N = \int_o^\infty I_F(t) \, dt.$$

Knowledge of ϕ and M is equivalent to knowledge of the functions S and G which correspond to the sine and cosine fourier transforms of the ideal pulse response $I_F(t)$. Consequently the measurement of phase and modulation as a function of the frequency

is equivalent to determining the time evolution of the emitting system to delta pulse excitation. In phase-modulation fluorometry, however, deconvolution for the finite width of the excitation pulse and the time response of the detection system is unnecessary since the ideal pulse response is obtained.

If the fluorescence decay is monoexponential then

$$\tan \phi = \omega\tau \tag{9}$$

and

$$M\ (1 + \omega^2\tau^2)^{-1/2}. \tag{10}$$

Another advantage of phase-modulation fluorometry is that it allows direct differential measurements. The general equations related to differential phase fluorometry have been given by Weber[6] and are applicable to a number of cases such as rotational studies and excited state reactions. As an example we discuss here its application to the determination of the time decay of the anisotropy.

In the time domain the anisotropy (r) is given by the following expressions,

$$r(t) = \frac{I_{\parallel}(t)-I_{\perp}(t)}{I_F(t)} \tag{11}$$

$$I_F(t) = I_{\parallel}(t) + 2I_{\perp}(t) \tag{12}$$

where $I_{\parallel}$ and $I_{\perp}$ represent intensities observed through polarizers oriented parallel and perpendicular, respectively, to the polarization plane of the exciting light (which is typically vertical).

The function r(t) can also be expressed as a sum of exponentials.[7,8] In the frequency domain the phase delay Δ and modulation ratio, Λ, between the parallel and perpendicular components of the fluorescence are measured. The corresponding

analytical expressions which relate the measurable quantities to the physical quantities of the system can be obtained from equations (4) and (5)[6],

$$\Delta = \arctan \frac{S_\perp}{G_\perp} - \arctan \frac{S_\parallel}{G_\parallel} \tag{13}$$

$$\Lambda = \left(\frac{S_\parallel^2 + G_\parallel^2}{S_\perp^2 + G_\perp^2} \right)^{1/2} . \tag{14}$$

We should note that the modulation ratio involves only the ratio of the AC components and not the ratio of the complete modulation terms.

Inverting equations (11) and (12) we obtain

$$I_\parallel = \frac{1}{3} I_F(t)[1 + 2r(t)] \tag{15}$$

$$I_\perp = \frac{1}{3} I_F(t)[1 - r(t)] \tag{16}$$

and

$$S_\beta = \int_o^\infty I_\beta(t) \sin \omega t \, dt \tag{17}$$

$$G_\beta = \int_o^\infty I_\beta(t) \cos \omega t \, dt \tag{18}$$

where β stands for either the parallel or perpendicular component. Notice again that relations 15 to 18 imply delta function excitation.

3. MODULATION OF THE EXCITING LIGHT

The two main sources of high repetition rate tunable pulsed light are electron storage rings which produces Gaussian pulses of synchrotron radiation and mode-locked lasers which output Lorentzian pulses. Gratton et al[9] have described a multifrequency cross-correlation phase fluorometer utilizing synchrotron radiation as a modulated light source. Other applications of

phase techniques in conjunction with synchrotron radiation have been reported[10,11] but in these reports only one or two harmonic frequencies were employed and cross-correlation techniques were not utilized. Pulsed laser excitation has also been utilized in phase fluorometry although details of instrumental design and capabilities in these cases are quite different from the present case.[12-15] In this section w discuss: (i) the harmonic content of both Gaussian and Lorentzian pulse shapes and (ii) the use of acousto-optic modulators to introduce variable harmonic content in pulsed light.

Equation (19) defines a Gaussian train of pulses spaced in time by a period T = 1/f,

$$Ga(t) = \sum_{n=-\infty}^{\infty} e^{-\left(\frac{t-nT}{a}\right)^2} . \tag{19}$$

The full width of the pulse at the half maximum (FWHM) is $\Delta t = 2a(\ell n 2)^{1/2}$. Figure 1a shows such a train of Gaussian pulses. In the frequency domain the fourier transform (convolution theorem) of Ga(t) leads to equation (2),

$$Ga(\omega) = \sqrt{2}\, a\, e^{\frac{-a^2\omega^2}{4}} \sum_{n=0}^{\infty} \delta(\omega - n\omega_o) \tag{20}$$

where $\omega_o = 2\pi/T$. Figure 1b shows the correspondence of figure 1a in the frequency domain; the sinusoidal signals are equally spaced in frequency by f = 1/T and convoluted by a Gaussian envelope of -3dB bandwidth point given by

$$f_G = \frac{2\ \ell n\ 2}{\pi(\Delta t)} . \tag{21}$$

Similarly, equation (22) defines a Lorentzian train of pulses spaced in time by a period T = 1/f and FWHM $\Delta t = 2b$,

$$L(t) = \sum_{N=-\infty}^{\infty} [b^2 + (t-nT)^2]^{-1} . \tag{22}$$

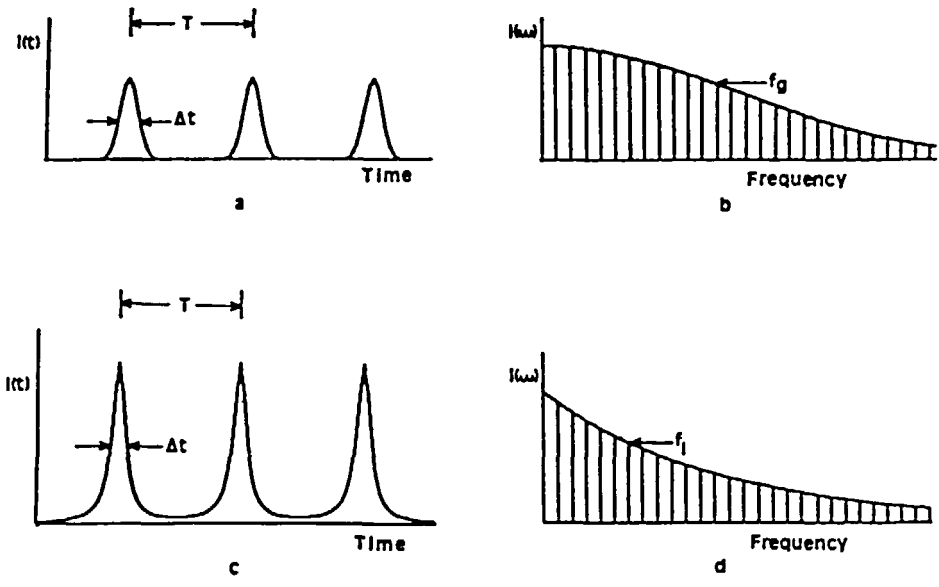

FIGURE 1

a) Train of Gaussian pulses of width Δt spaced a time T in the time domain; b) Correspondence of figure 1a in the frequency domain; c) Train of Lorentzian pulses of width Δt spaced a time T in the time domain; d) Correspondence of figure 1c in the time domain.

Figure 1c shows such a pulse train. The convolution theorem leads to the frequency domain representation of L(t),

$$L(\omega) = \frac{2\pi\, e^{-b\omega}}{b} \sum_{n=0}^{\infty} \delta(\omega - n\omega_o). \tag{23}$$

Figure 1d provides the frequency domain correspondence of figure 1c, and shows a set of frequencies equally spaced by f convoluted with an exponential envelope of -3dB frequency bandwidth given by

$$f_L = \frac{\ell n 2}{\pi(\Delta t)}. \tag{24}$$

Notice that $f_G = 2f_L$. Hence, for the same FWHM, synchrotron radiation provides twice the harmonic content of mode-locked lasers. However, much narrower pulses are obtainable from lasers. Gratton et al[9] used synchrotron radiation pulses of approximately 2 nanosecond FWHM which corresponds to a -3dB frequency bandwidth of 220 MHz. The pulsewidth of the present instrument is less than 100 ps which corresponds to a -3dB frequency bandwidth of 2200 MHz. Pulses which are narrower still by a factor of ten (i.e., 10 psec) are not difficult to achieve using commercial synchronously pumped dye lasers. In figures 1b and 1d one notes that the harmonics of very narrow pulses have the same light intensity as the zero frequency harmonic. The zero frequency harmonic in turn corresponds to the average intensity of the light signal. Therefore in the frequency domain all the photons in the light pulse fully contribute to the measurements at each frequency. The average signal measured at the nth harmonic $I(n\omega)$ for very narrow pulses has practically the same intensity as the complete fluorescence signal, $\langle F(t) \rangle$.[9]

The frequency spacing of the output from mode-locked lasers is too large for practical phase and modulation fluorometry experiments which must handle a wide range of fluorescence lifetimes and rotational rates. Other frequencies between the laser harmonics can, however, be introduced by amplitude modulation of the pulsed laser output. Figure 2 shows the amplitude modulation of the train of pulses from a dye laser by an acousto-optic modulator. Amplitude modulation of the train of pulses from the dye laser introduces two additional frequencies around each harmonic as shown in figure 3, in which the actual frequency response of the modulated dye laser pulse train was resolved using a 1.8 GHz frequency analyzer (Tektronics Model L-14) and a fast photodiode (Lasermetrics model 3117). The new set of frequencies available after the amplitude modulation are nf, nf + 2k and nf - 2k (figure 3) where the frequency k can be varied quasi-continuously and corresponds to the frequency at which the acousto-optic modulator crystal is driven and f is the repetition

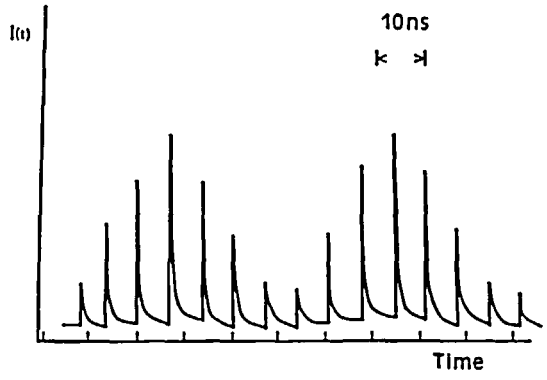

FIGURE 2

Amplitude modulation of the pulse train by the acousto-optic modulator in the time domain.

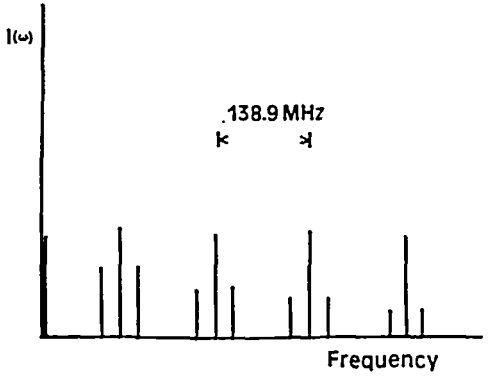

FIGURE 3

Introduction of additional harmonics between the laser harmonics by amplitude modulation of the pulsed beam in the frequency domain.

rate of the mode locked laser (138.9 MHz in our present instrument). The harmonics of the laser pulses used is defined by $n = 0, 1, 2, \ldots$. Variation of the frequency k continuously from 34.5 MHz to 69.5 MHz allows us to obtain all the frequencies from DC to several GHz. The frequency applied to the mode-locker head crystal equals half the pulse repetition rate. For reasons of convenience both the acousto-optic modulator and the mode-locker head should have the same nominal resonant frequency; such an arrangement allows for a continuous sweep of frequencies without gaps.

The fluorescence of a sample stimulated by such amplitude modulated light contains all the modulation frequencies present in the exciting light up to a few GHz. The maximum frequency at which a fluorescent molecule can respond is limited by its lifetime; higher frequencies in the fluorescence signal are attainable with shorter fluorescence lifetimes. For each frequency there exists a corresponding phase delay and modulation given by equations (4) and (5). Cross-correlation techniques are employed in the present work in order to isolate the phase and modulation information contained in a given frequency.

4. THE CROSS-CORRELATION PRINCIPLE

The fluorescence signal from the sample, F(t), given by equation (3) is detected by a photomultiplier tube. The response of the present instrument detector (PMT) to the fluorescence signal is also given by F(t) in the DC-1GHz frequency range (see the PMT section). The principle of operation of a cross-correlation phase and modulation fluorometer has been previously described.[16,17] The method consists of amplitude modulation of the detector gain by a sinusoidal voltage C(t)

$$C(t) = C_o[1 + M_c\cos(\omega_c t - \phi_c)]. \qquad (25)$$

In our instrument the modulation of the detector is performed by applying C(t) to the second dynode of the PMT. The frequency ω is

just slightly different from the main modulation frequency. The low frequency terms of the modulation product F(t)C(t) given by

$$F(t)C(t) = F_o C_o \left[1 + \frac{M_F M_C}{2} \cos(\Delta\omega t - \Delta\phi)\right] \qquad (26)$$

where $\Delta\omega = \omega_c - \omega$ and $\Delta\phi = \Delta\phi_c - \phi$ can be filtered out from the rest of the signal. Notice that the term of frequency $\Delta\omega$ contains all the phase and modulation information of the original fluorescence signal. In the present instrument, $\Delta f = \frac{\omega}{2\pi} = 31$ HZ.

5. DESCRIPTION OF THE INSTRUMENT

The present instrument is a modified version of the phase and modulation fluorometer described previously.[4]

Figure 4 shows the overall layout of the instrument. The whole system is mounted on a Newport Research Corp. MST-10 NRC honeycomb non-isolated optical table.

The light source is the green line (514.5 nm) from an argon ion laser (Spectra Physics model 164/9) mode locked at 138.9 MHz using a 69 MHz Spectra Physics mode-locker head. The mode-locker head temperature controller is a modified INRAD model 5-011A temperature controller.

The ion laser synchronously pumps a cavity extended dye laser (Spectra Physics 375). The output light wavelength from the dye laser is selectable by moving a tuning wedge along the beam which gives a 0.3 nm linewidth (specified by the manufacturer). Once the wedge has been adjusted a narrower linewidth can be obtained using a fine etalon (a 0.06 nm linewidth is specified by the manufacturer). Using rhodamine 6G a continuous spectrum is obtained between 560 nm and 630 nm. Using DCM, 625 nm to 680 nm range is obtained and oxazine 1 gives the 675 nm to 780 nm range. Other dyes can also be used with acceptable performance. All the dyes used were from Exciton.

The train of pulses from the dye laser is amplitude modulated by means of a quartz acousto-optic modulator (Intra-Action ML72Q) as shown in figure 2. The acousto-optic modulator resonant frequencies are spaced at 0.331 MHz; the useful range of this modulator is from 35 MHz to 70 MHz. The temperature coefficient

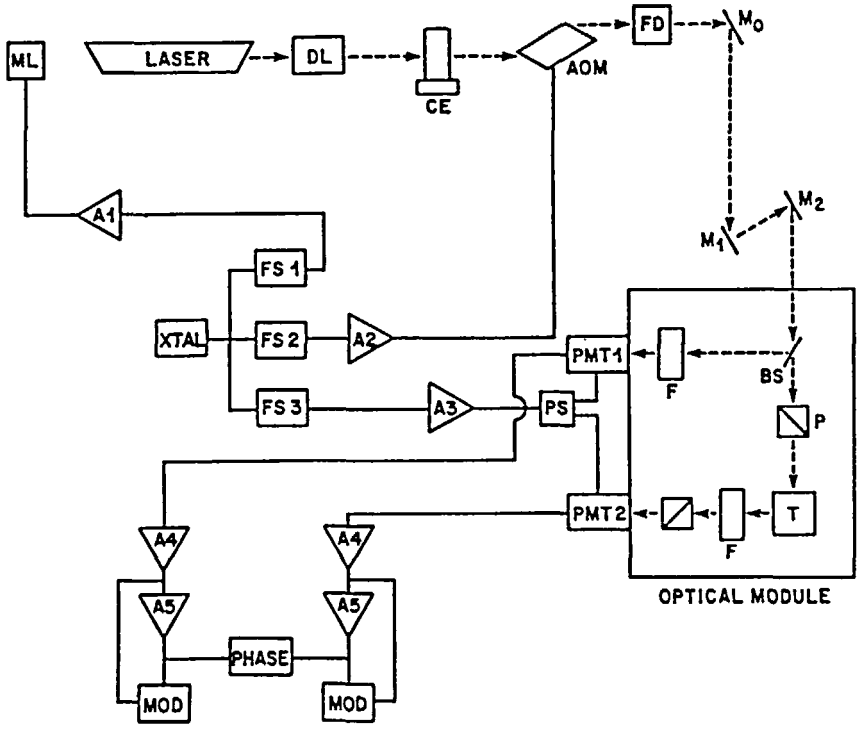

FIGURE 4

Layout of the instrument. ML = 69 MHz Spectra Physics Mode-Locker head; Laser = Spectra Physics model 164-9 argon ion laser; DL = dye laser Spectra Physics model 375; CE = linear translator NRC model 420; AOM = Acousto-optic Modulator Intra-Action model ML-72Q; FD = Frequency doubler Spectra Physics model 390-01; BS = Quartz beam splitter; FS1 = Rockland 560 frequency synthesizer, FS2 = PTS 500 frequency synthesizer; FS3 = HP 8662A frequency synthesizer; XTAL = 10 MHz quartz oscillator; A1, A2 = ENI 411LA RF amplifier; A3 = ENI 603L RF amplifier; PS = power splitter; T = sample; F = Filter holder; P = polarizer; PMT1, PMT2 = Hamamatsu R928 photomultiplier tubes; A4 = DC amplifier; A5 = AC tuned amplifier; PHASE = digital phase meter; MOD = digital ratio voltmeter; M0,M1,M2 = UV mirrors.

of the crystal resonant frequencies is about 7KHz/C. At 40 MHz the width of each of the resonant frequencies is about 5 KHz. A water bath temperature controller was used to fix the crystal temperature within 0.1C which thus corresponds to approximately 2 KHz or 1/3 of the resonance width. To vary the frequency from 35 MHz to 70 MHz the tuning circuit provided with the modulator was removed and the RF power applied to the crystal was about 5 W using a 50 ohm terminator placed close to the crystal. The efficiency of the acousto-optic modulator as specified by the manufacturer is about 50%.

The amplitude modulated train of visible light from the acousto-optic modulator is frequency doubled to UV light using a Spectra Physics Model 390-01 angle tuned frequency doubler. The manufacturer provides two different crystals to work in different wavelength ranges; KDP for 280 nm to 340 nm and $LiIO_3$ for the 330 nm to 440 nm range. The non-linear nature of the doubling process improves the amplitude modulation of the light beam. This configuration gave a signal which was stable over a period of several days.

The polarization of the dye laser light is vertical relative to the laboratory axis while the UV output from the doubler is horizontally polarized. The plane of polarization of the UV beam was rotated to 35 degrees from the vertical (ideal polarization for lifetime measurements[18]) using an arrangement of two mirrors. The mirrors, which not only change the polarization plane of the exciting light but also steer the beam into the sample module, have a metallic coating (Melles Griot coating 028); a dielectric coating would give rise to a wavelength and polarization dependent reflection.

A. THE PHOTOMULTIPLIER CIRCUIT

The Hamamatsu R928 photomultiplier tube was selected because of its wide-range wavelength sensitivity, low price and relatively small color effect.[9]

The photomultiplier circuit, shown in figure 5, is composed of a resistor chain divider and a circuit for RF modulation. The

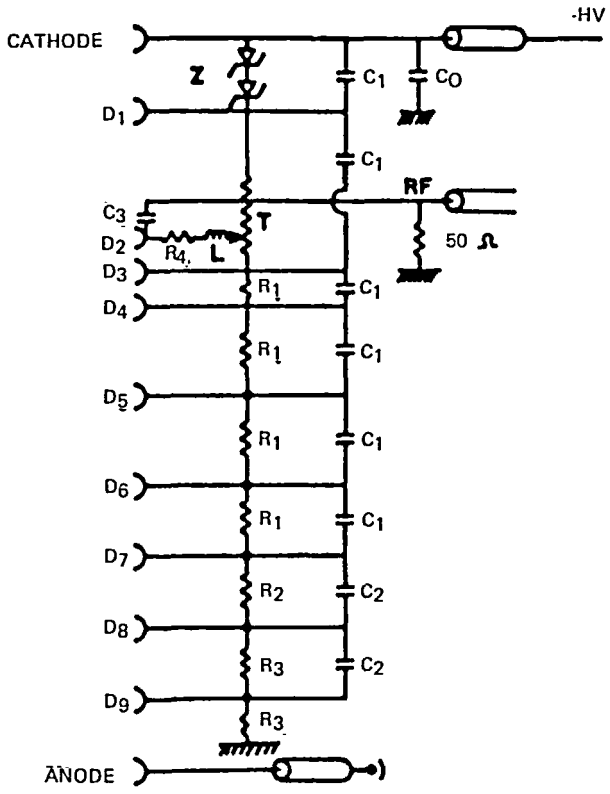

FIGURE 5

Photomultiplier circuit Z = 75V zener diode IN4765A, C_o = 1000 pF, 6KV, C_1 = 5 nF, C_2 = 10 nF, T = 250 KΩ, R_1 = 82 KΩ, R_2 = 110 KΩ, R_3 = 160 KΩ, R_4 = 10 KΩ, L = 1 mH.

modulation is obtained by application of an alternating voltage to the second dynode D2. In figure 6, we show the output current at the anode under the condition of constant cathode illumination as a function of the voltage applied to the 2nd dynode. One notes that the characteristic curve has a sharp rise, then the current reaches a maximum and decays again as the absolute voltage of the dynode increases. In order to modulate the gain of the PMT an RF voltage of about 40V peak to peak is needed corresponding to an

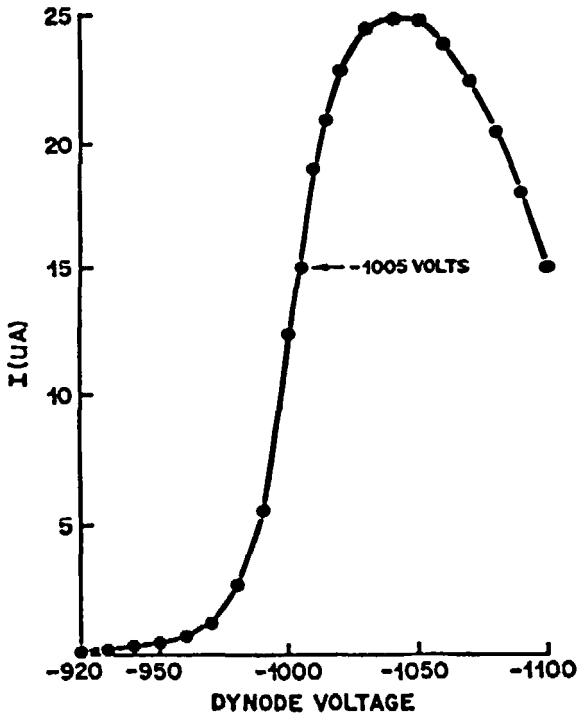

FIGURE 6

Dynode characteristic curve.

average power of 4W on a 50 ohm terminator. The center voltage of about -1005V is set using the trimpot of the photomultiplier circuit to obtain the best photomultiplier output modulation. The RF voltage is provided by an RF amplifier, ENI Model 603L. This amplifier can deliver up to 3W linearly (5W non-linear) in the 0.8 MHz-1000 MHz frequency range. The value of the zener diode Z has been chosen in order to minimize color effects having the maximum acceleration voltage compatible with the tube specifications.

The frequency response of the photomultiplier circuit to modulated light is determined by the frequency response of the

cathode and the first two dynodes. The cross-correlation performed in the second dynode transfers the phase and modulation information of the high frequency signals to 31 HZ.[16]

B. THE ELECTRONIC DETECTION SYSTEM

In figure 7 we report a block diagram of the electronics. The output of the two photomultiplier tubes is analyzed separately by two identical channels. In the following discussion we describe the operation of only one of these channels.

After an initial amplification stage (A1) the signal is separated into AC and DC components. The DC component is integrated (I) in order to generate a DC signal proportional to the average intensity of the detected signal. The AC component is amplified (A2) and filtered by a band pass active filter (F) to select the 31 HZ component. The output of the filter is rectified (R) and integrated (I) to produce a continuous voltage proportional to the amplitude of the 31 Hz AC component. The filter is tuned at 31 Hz with a Q of approximately 200 (figure 8). The DC and AC parts of each channel are continuouslyl monitored by four digital voltmeters. These voltmeter readings are not utilized for data acquisition but only for rapid inspection of the signal levels. An ISS1 interface connected to an IBM PC is used for accurate measurements of the volage amplitudes. The output of the two active filters (channel 1 and channel 2) are sent to zero crossing detectors (Z) where two square waves are produced. The ISS interface uses the positive going edge of the square waves to start and stop a phase counter built in the ISS card. The clock input of the phase counter is 1 MHz. The content of the counter is proportional to the phase difference between the signals from the two channels. The resolution for phase measurements for 1 second integration is 1 microsecond which corresponds to an angular resolution of about 0.01 degrees. One may integrate phase readings for different integration periods, a typical integration period being 2 to 3 seconds. The digital values of the phase, AC and DC from the ISS1 interface are read and stored by the IBM PC

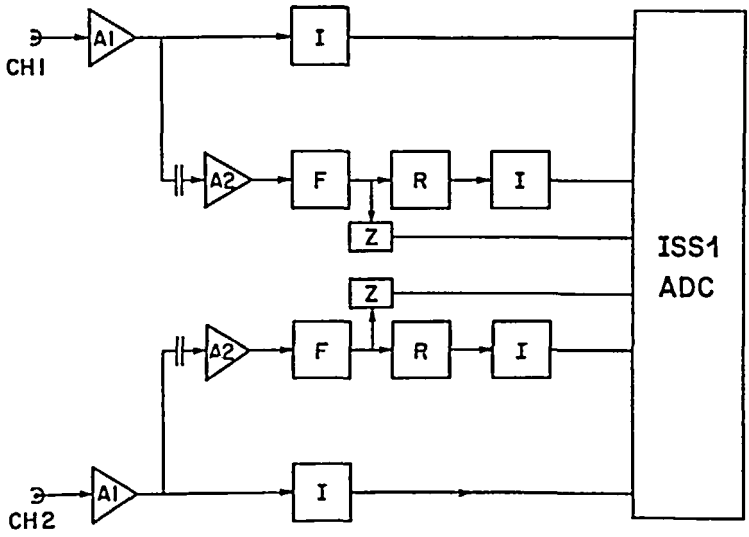

FIGURE 7

Block diagram of the electronics. A1, A2 = low frequency amplifier; I = integrator; F = narrow band pass filter tuned at 31 Hz; R = Rectifier; Z = zero-crossing detector.

for acquisition and data analysis of data. The software for data acquisition and analysis was provided by ISS, Inc.

C. CROSS-CORRELATION FREQUENCY GENERATION

The characteristics of our electronic detection system require that the frequency synthesizer used to generate the cross-correlation frequency at the PMT has a resolution of at least 1 Hz over the entire frequency range utilized; the two other frequency synthesizers may have less resolution (1 KHz). The phase noise of our synthesizers are -110dB at 1 KHz or better. In our instrument, the mode-locker head is driven by a frequency synthesizer (Rockland Systems Co. model 5600) with a frequency range of 0.1 Hz-160 MHz and resolution of 1 Hz. The acousto-optic modulator is driven by a PTS model 500 synthesizer with a 0.1 MHz-500 MHz frequency range and 0.1 Hz resolution. The frequency for

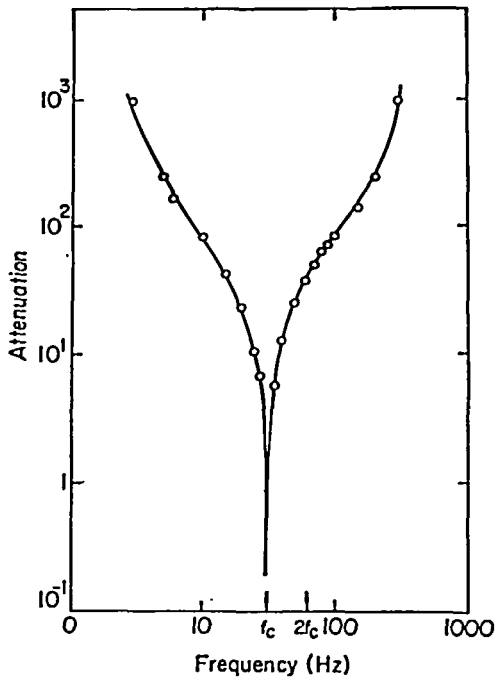

FIGURE 8
AC filter response.

modulation of the PMT response is generated by a Hewlett-Packard model 8662A frequency synthesizer with a range of 10 KHz-1275 MHz and 0.1 Hz resolution. These three synthesizers are locked to the same quartz crystal so that the signals are phase coherent over the entire frequency range. The phase noise, the only important parameter in this configuration, has been checked by sending the outputs from a pair of synthesizers to a mixer (Minicircuit ZAD 1) and measuring the period of the wave at 1 Hz. This period was constant to within four significant digits using an integration time of one second. No drift was observed over a period of two hours. The three synthesizers are not equipped with the high stability crystal option, which is an unnecessary feature since only the phase coherence of the three synthesizers is important.

D. SYSTEMATIC ERRORS AND SENSITIVITY OF THE INSTRUMENT

Gratton and Limkeman[4] have studied the systematic errors of phase and modulation fluorometers. Two main systematic errors have been reported. (i) Color effects due to the wavelength-dependent phase delay of the photocathode.[17] The importance of such effects in this instrument will be discussed in the results section. In fluorescence depolarization measurements color effects do not appear since the parallel and perpendicular components of the fluorescence are compared. (ii) Non-homogeneous modulation of the exciting light beam. Water tank acousto-optic modulators can introduce non-homogeneous modulation of the exciting beam.[17] In measurements taken using the quartz acousto-optic modulator described here no such systematic errors have been found.

The time resolution of the instrument is ultimately determined by the phase noise. For a total integration period of 20 seconds we typically find the standard deviation of the phase angle to be ±0.2 degrees. At 400 MHz this phase error corresponds to a time resolution of about 1 picosecond.

6. APPLICATIONS

A. LIFETIME ANALYSIS

Since the instrument was designed primarily for this study of the intrinsic emission of proteins we began by evaluating the instrument's performance using pure tryptophan in aqueous solution. Table I shows the lifetime obtained for tryptophan (Fluka) at 20°C in pH 6.0, 0.01M sodium phosphate buffer. The excitation wavelength was 300 nm (optical density at 300 nm was below 0.05) and the emission was observed through a Corning 0-52 filter (λ_{em} > 320 nm). One notes that a systematic lengthening of the apparent phase lifetime occurs at high frequencies. This lengthening is possibly due to a "color error" in the Hamamatsu R928 phototube which has not been investigated at frequencies above 200 MHz or a systematic error, as yet unspecified, maybe present. Similar results are shown in table I for a solution of p-terphenyl in cyclohexane using the same excitation wavelength and emission

TABLE 1

Lifetime Measurements

Tryptophan pH 6

J	F	TP	TM	P	M
1	7.200	3.020	3.571	7.780	0.987
2	19.200	3.070	3.374	20.320	0.926
3	43.200	3.026	3.216	39.400	0.753
4	86.300	2.806	3.056	56.690	0.517
5	138.900	3.029	3.041	69.280	0.353
6	158.100	3.120	2.974	72.120	0.321
7	297.100	3.713	2.782	81.790	0.189

p-Terphenyl in cyclohexane

J	F	TP	TM	P	M
1	7.200	0.954	2.128	2.470	0.995
2	19.200	0.956	1.692	6.580	0.980
3	43.200	1.016	0.641	15.420	0.985
4	95.800	1.034	0.902	31.900	0.879
5	138.900	1.095	0.909	43.700	0.783
6	182.100	1.155	0.885	52.880	0.703
7	234.700	1.235	0.872	61.230	0.614
8	321.000	1.228	0.797	68.010	0.528
9	416.800	1.226	0.872	72.700	0.401

Tryptophan vs. p-terphenyl

J	F	TP	TM	P	M
1	43.200	3.071	3.199	39.810	0.755
2	95.800	3.027	3.127	61.240	0.469
3	138.900	3.004	3.123	69.120	0.344
4	182.100	3.000	3.142	73.760	0.268
5	234.700	2.792	3.092	76.350	0.214
6	321.000	2.475	3.026	78.670	0.162

Lysozyme vs. p-terphenyl

J	F	TP	TM	P	M
1	25.200	2.747	4.112	23.510	0.838
2	43.200	2.456	3.483	33.690	0.727
3	95.800	2.067	2.853	51.210	0.503
4	138.900	1.880	2.807	58.640	0.378
5	182.100	1.823	2.570	64.390	0.322
6	234.700	1.799	2.436	69.350	0.268
7	277.900	1.721	2.391	71.590	0.233
8	321.000	1.532	2.314	72.070	0.209

Excitation 300 nm, Emission coming 0-52 filter, F = frequency in MHz, TP = phase lifetime in nsec, TM = modulation lifetime in nsec, P = phase in degrees, M = modulation.

TABLE 2

Least-squares analysis

Tryptophan

COMPONENT	LIFETIME	FRACTION	ALPHA
1	3.037±0.051	1.000	1.000
COMPONENT	LIFETIME	FRACTION	ALPHA
1	17.582±66.741	0.015±0.041	0.003
2	3.006± 0.100	0.985	0.997

p-Terphenyl

COMPONENT	LIFETIME	FRACTION	ALPHA
1	1.055± 0.038	1.000	1.000
COMPONENT	LIFETIME	FRACTION	ALPHA
1	2.217± 3.848	-0.303±1.546	-0.149
2	1.233± 0.396	1.303	1.149

Tryptophan vs. p-terphenyl

COMPONENT	LIFETIME	FRACTION	ALPHA
1	3.041± 0.039	1.000	1.000
COMPONENT	LIFETIME	FRACTION	ALPHA
1	3.117± 0.033	0.996±0.002	0.630
2	0.023±0.709	0.004	0.370

Lysozyme vs. p-terphenyl

COMPONENT	LIFETIME	FRACTION	ALPHA
1	2.252± 0.134	1.000	1.000
COMPONENT	LIFETIME	FRACTION	ALPHA
1	4.760± 0.473	0.558±0.058	0.267
2	1.374± 0.092	0.442	0.733
COMPONENT	LIFETIME	FRACTION	ALPHA
1	11.369± 4.811	0.177±0.079	0.035
2	2.606± 0.444	0.675±0.048	0.590
3	0.896± 0.195	0.148	0.375

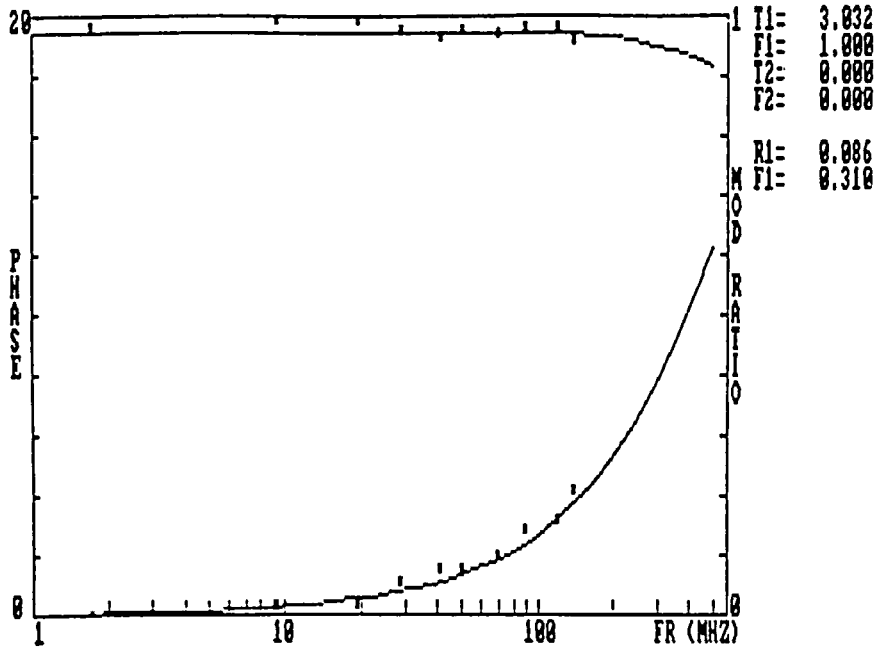

FIGURE 9

Tryptophan in water. Differential phase and modulation ratio as a function of frequency. Excitation at 300 nm, emission seen using a Corning 0-52 filter. T = 20°C. T = lifetime in nanosecond, R = rotational correlation time in nanosecond, F = fractional intensity.

filter. Again one notes a systematic lengthening of the apparent phase lifetime at the higher modulation frequencies. However, when the tryptophan lifetime is measured using p-terphenyl as a reference (using τ = 1.0 nsec) instead of a scatter solution this lengthening effect disappeared as shown in table I.

A non-linear least squares analysis of the tryptophan lifetimes using 1 or 2 exponential components gave the results tabulated in table II. A similar lifetime study was undertaken on lysozyme (from egg white) also using p-terphenyl as a reference standard.

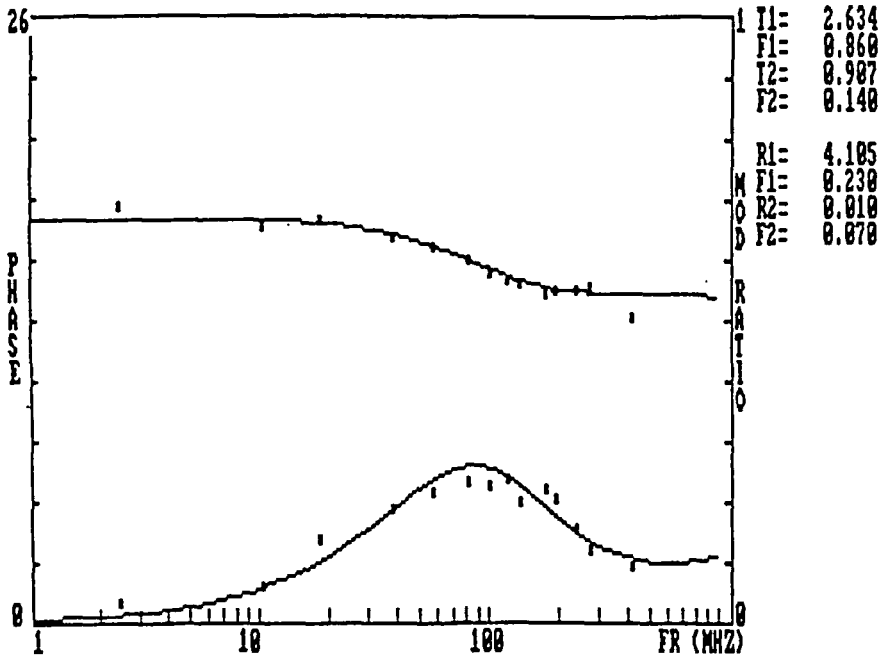

FIGURE 10

Lysozyme in phosphate buffer. Differential phase and modulation ratio as a function of frequency. Excitation at 300 nm, emission seen using a Corning 0-52 filter. T = 20°C. T = lifetime in nanoseconds, R = rotational correlation time in nanoseconds, F = fractional intensity.

The measured lifetimes are given in table I and the results of the heterogeneity analysis are shown in table II.

B. ROTATION ANALYSIS

The differential tangent and modulation ratio for a solution of tryptophan at pH 6 was measured. The non-linear least-squares analysis in terms of a single isotropic rotator gives a rotational rate of 86 ps. The results are shown in figure 9. It is clear from our measurements that such a fast rotation can be accurately determined with our apparatus. We report also in figure 10 the

measurements for the rotations of lysozyme in phosphate buffer. In this later case the rotational motion appears more complex. Work is in progress to determine the nature of the rotational motions in proteins.

ACKNOWLEDGEMENTS

We would like to thank Dr. Frank Prendergast for his help in acquiring some of the equipment and for valuable discussions concerning the preparation of this manuscript. We are grateful to Dr. Henry Merkelo for his suggestions on the design of the PMT circuitry and to Mr. Gerald Marriott for his assistance in some of the data acquisition. We would also like to thank Spectra Physics for providing the 390 frequency doubler and the 69 MHz mode-locker head.

This work was possible thanks to the financial support to E.G. from a National Science Foundation grant PCM 84-03107 and a Naval Research grant MDA 903-85-X-0027. D.M.J. wishes to acknowledge a National Science Foundation grant PCM 84-02663 and a Robert A. Welch Foundation grant I-986.

REFERENCES

1. A. Grinwald and I. Z. Steinberg, Biochim. Biophys. Acta 427, 663 (1976).
2. J. Longworth, "Time Resolved Fluorescence Spectroscopy in Biochemistry and Biology," R. B. Cundall and R. E. Dale, Eds., NATO ASI Series A, Life Sciences Vol. 69A, Plenum, New York, 1983, p. 651.
3. J. M. Beechem and L. Brand, Ann. Rev. Biochem. 54, 43 (1985).
4. E. Gratton and M. Limkeman, Biophys. J. 44, 315 (1983).
5. M. G. Badea and L. Brand, Methods Enzymol 61, 378 (1979).
6. G. Weber, J. Phys. Chem. 85, 949 (1981).
7. A. Szabo, J. Chem. Phys. 81, 150 (1984).
8. A. J. Cross, D. H. Waldeck and G. R. Fleming, J. Chem. Phys. 78, 11 (1983).
9. E. Gratton, D. M. Jameson, N. Rosato and G. Weber, Rev. Sci. Instrum. 55, 486 (1984).

10. A. P. Sabersky and I. H. Munro, "Picosecond Phenomena," C. V. Shank, Ed., Springer, New York, 1979.
11. P. Sebban and I. Moya, Biochim. Biophys. Acta 722, 436 (1983).
12. G. M. Hieftje, G. R. Haugen and J. M. Ramsey, Appl. Phys. Lett. 30, 463 (1977).
13. G. M. Hieftje and E. E. Vogelstein, "Modern Fluorescence Spectroscopy" Vol. 4, E. L. Wehry, Ed., Plenum, New York, 1981.
14. H. Merkelo, S. Hartman, T. Mar, G. S. Shinghal and Govindjee, Science (Wash. D.C.) 164, 301 (1969).
15. F. E. Lytle, M. J. Pelletier and T. D. Harris, Appl. Spectrosc. 33, 28 (1979).
16. R. D. Spencer and G. Weber, Ann. N.Y. Acad. Sci. 158, 361 (1969).
17. D. M. Jameson, E. Gratton and R. D. Hall, Appl. Spectros. Rev. 20, 55 (1984).
18. R. D. Spencer and G. Weber, J. Chem. Phys. 52, 1654 (1970).